Paper presented at the 22nd Asian Conference on Remote Sensing, 5 - 9 November 2001, Singapore.

SUN GLITTER IN SPOT IMAGES AND THE VISIBILITY OF OCEANIC PHENOMENA

Christian MELSHEIMER, KWOH Leong Keong
Centre for Remote Imaging, Sensing and Processing,
Faculty of Science, National University of Singapore,
Blk SOC-1, Lower Kent Ridge Road, Singapore 119260
Tel: (+65) 8746587, Fax: (+65) 7757717
E-mail: crscm@nus.edu.sg
SINGAPORE

KEY WORDS: SPOT, Sun Glitter, Ocean Surface

ABSTRACT: In this paper we study the effect of sun glitter on the imaging of the ocean by optical satellite sensors. Sun glitter is the specular reflection of sunlight by suitably tilted facets of the water surface into the sensor, therefore the intensity of sun glitter depends on the ocean surface roughness and on the imaging geometry (sun's position, sensor's viewing direction). It is the effect of sun glitter that makes oceanic phenomena like surface slicks or current gradients visible on images from, e.g., the SPOT (Satellite Pour l'Observation de la Terre) or Landsat satellites. The relation between surface roughness, imaging geometry and sun glitter is non-trivial and knowledge of it is relevant for correctly interpreting optical satellite images.

1. INTRODUCTION

In satellite images by optical sensors, e.g. the HRV (High Resolution Visible scanner) aboard the SPOT (Satellite Pour l'Observation de la Terre) satellites, mesoscale oceanic phenomena such as internal waves, surface slicks, and current gradients are sometimes distinctly visible and sometimes not visible at all. Furthermore, the signatures can "change sign", i.e., they can look either bright or dark. An example for this is shown in Figures 1 and 2 which both show oil slicks as seen by SPOT. The reason is that these phenomena modulate the surface roughness which in turn modulates the sun glitter pattern of the water surface. Sun glitter is the specular reflection of sunlight by suitably tilted facets of the water surface into the sensor. Optical sensors are sensitive to sun glitter - and thus to those oceanic phenomena that modify the surface roughness - if the imaging geometry (i.e., sun's position in the sky, sensor's viewing direction) is suitable.

In the following, we investigate the relationship between the imaging geometry and the visibility of oceanic phenomena in SPOT images, based on the standard model for the sun glitter radiance of the water surface. It is a little known fact that actually the dependence of the sun glitter radiance on the surface roughness (mean square slope) is not monotonic, but instead has a maximum. The position of the peak depends on the scene geometry. The consequence is that

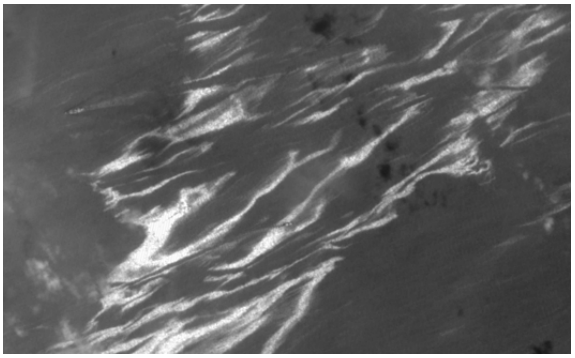

Figure 1: Part of a SPOT panchromatic image, 11 Oct 2000, 03:45:44 UTC, a few km south of Singapore. The bright lines are oil slicks that were caused by an oil tanker accident on 03 Oct, 2000, in the Singapore Strait. © CNES 2000

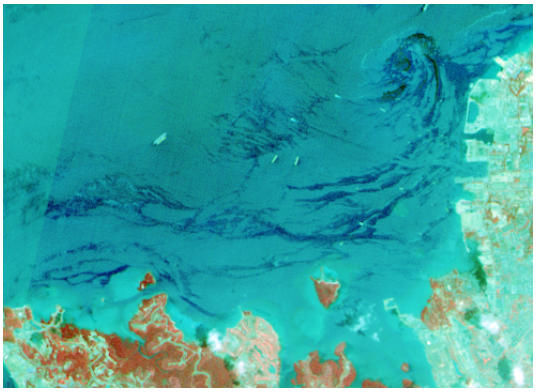

Figure 2: Part of a SPOT multispectral image, 08 Oct 2000, 03:35:10 UTC, near Batu Ampar, Indonesia, just south of the Singapore Strait. Here, dark lines and filaments are oil slicks that were caused by the same tanker accident mentioned in the caption of the figure on the left. © CNES 2000

smooth areas appear brighter than rough areas or vice versa. Moreover, it is possible that the sun glitter is negligible, so that the radiance measured by the sensor is dominated by the light reflected and scattered from the water column and the bottom. In this case, the above-mentioned oceanic phenomena are invisible.

Knowledge about the dependence of sun glitter on the scene geometry is therefore relevant for the correct interpretation of SPOT images showing oceanic phenomena such as internal waves, surface slicks, and current gradients, as well as for assessing the best viewing condition for these phenomena.

2. SUN GLITTER RADIANCE AND OCEAN SURFACE ROUGHNESS

As stated above, sun glitter is the specular reflection of sunlight into the sensor by facets of the water surface that are suitably tilted. Thus the surface wave spectrum, or the surface roughness, as well as the viewing geometry of the image determine the sun glitter radiance. It can dominate the radiance received from the water if the viewing direction of the sensor is within about 20° of the direction of sunlight reflection from a flat water surface. The sensor does not, of course, see the individual highlighted facets (as the human observer on the beach or a ship does), but the average over a resolution cell which has, in the case of the HRV of SPOT, a size of 20 m by 20 m. The more facets with the suitable slope values there are, the stronger the sun glitter radiance received by the sensor. The probability of occurrence of such facets is closely related to the probability distribution function of slopes (Cox and Munk, 1954; Zeisse, 1995); where slope means the partial derivatives with respect to x and y of the surface elevation $z(x, y)$, z_x and z_y. Following the comprehensive analysis of Zeisse (1995), we obtain for the sun glitter radiance N_{sg} received by a sensor with an (off-nadir) viewing angle* θ of less than 80°(SPOT: $\theta \leq 35°$):

$$N_{sg} = H_{\odot} \frac{1}{4} p(\hat{z}_x, \hat{z}_y) [\cos \hat{\beta}]^{-4} [\cos \theta]^{-1} \rho(\hat{\omega}) \tag{1}$$

where $H_{\odot}$ is the solar irradiance at the sea surface, $\hat{\beta}$, $\hat{z}_x$, and $\hat{z}_y$ are the surface tilt angle (off-horizontal) and the slope components required for specular reflection of sunlight into the sensor; $p(z_x, z_y)$ is the probability distribution function of the slopes; $\hat{\omega}$ is the reflection angle for specular reflection of sunlight into to sensor, $\rho(\hat{\omega})$ is the Fresnel reflection coefficient of the water surface. The probability distribution function of the slopes (slope pdf) can be approximated as a Gaussian with the mean square slope σ^2 as width parameters (Cox and Munk, 1954):

$$p(z_x, z_y) = \frac{1}{\pi \sigma^2} \exp \left[- \frac{z_x^2 + z_y^2}{\sigma^2} \right] \tag{2}$$

Actually, if the surface roughness is caused by a steady wind, the slope pdf is slightly asymmetric, and Cox and Munk (1954) have derived an empirical relationship between the wind speed and the mean square slopes in up/downwind and crosswind direction. However, if the roughness is influenced by current gradients or by surface slicks, there is no simple scalar relationship that gives the mean square slope, but instead, hydrodynamical modeling of the surface wave spectrum is required, which is beyond the scope of this paper (some information on that can be found in Melsheimer et al., 2000). Therefore we shall use the mean square slope σ^2 as the main parameter for the surface roughness. We may also use the empirical relationship between wind speed and mean square slope for the symmetric approximation of the slope pdf (also by Cox and Munk, 1954) just to translate the abstract mean square slope into a more palpable wind speed ($\sigma^2 = 0.003 + 5.12 \times 10^{-3} W \pm 0.004$, where W is the wind speed in m/s) even though the roughness might not be caused by wind only.

Equation (1) mixes the slopes $\hat{z}_x$, $\hat{z}_y$ and the angle $\hat{\beta}$ that are required for specular reflection of sunlight into the sensor, although they are related by $\tan^2 \hat{\beta} = \hat{z}_x^2 + \hat{z}_y^2$. Using this and substituting equation (2) into equation (1), writing it as a function of the "roughness parameter" σ^2 (the mean square slope), and dividing by the sun's irradiance $H_{\odot}$ for normalization purposes, we finally get the (relative) sun glitter radiance

$$N_{rel.sg}(\sigma^2)/H_{\odot} = \frac{1}{4} \rho(\hat{\omega}) \frac{1}{\pi \sigma^2} \exp \left[- \frac{\tan^2 \hat{\beta}}{\sigma^2} \right] [\cos \hat{\beta}]^{-4} [\cos \theta]^{-1} \tag{3}$$

This is the equation we need in order to interpret a given image: For a given scene geometry, i.e., sensor's viewing direction and the sun's position in the sky, we can calculate the tilt angle $\hat{\beta}$ that would be needed for specular reflection of sunlight into the sensor, as well as the corresponding reflection angle $\hat{\omega}$ (see equations in Appendix). Thus we get the sun glitter radiance as a function of the surface roughness (mean square slope) for the given scene and can examine

*often called incidence or incident angle

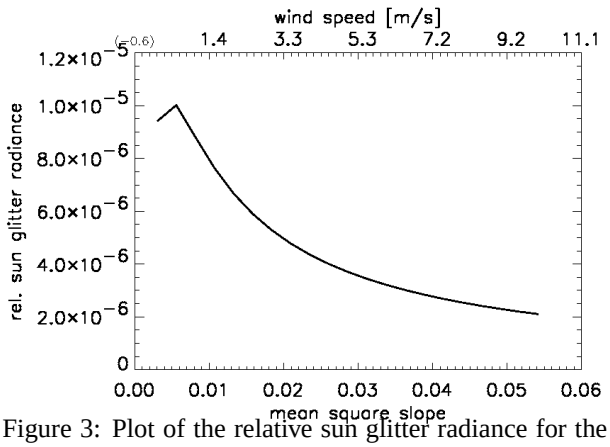

Figure 3: Plot of the relative sun glitter radiance for the SPOT image with bright-looking oil slicks in Figure 1 (11 Oct 2000, 03:45:44 UTC); $\hat{\beta} = 3.7°$.

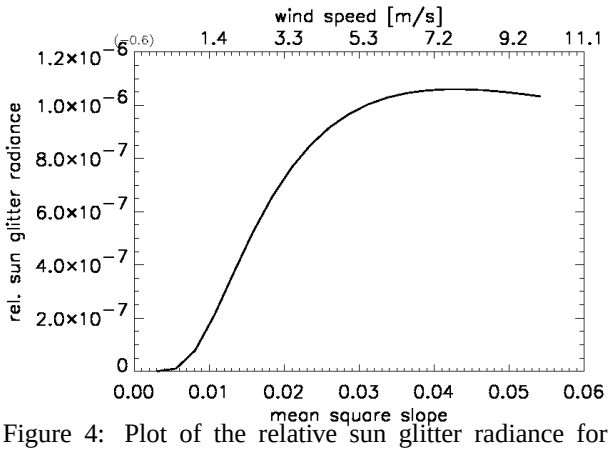

Figure 4: Plot of the relative sun glitter radiance for the SPOT image with dark-looking oil slicks in Figure 2 (08 Oct 2000, 03:35:10 UTC); $\hat{\beta} = 11.7°$.

the behavior of that function. Simple analysis shows that $N_{rel.sg}$ as in equation (3) has a maximum for $\sigma^2 = \tan^2 \hat{\beta}$. Therefore, just calculating $\hat{\beta}$ from the scene geometry gives an idea of the shape or the sun glitter radiance curve.

If the maximum is at very low roughness, $N_{rel.sg}$ will decrease for higher roughness, which means that the image is the darker, the rougher the water surface is. If the maximum is at high roughness values (near the upper end of the range that can be expected to occur), $N_{rel.sg}$ will be increasing in the range of realistic roughness values which means that the image is the brighter, the rougher the water surface is. Note that the spatial variations of θ and ζ within one SPOT scene (60 km by 60 km) are less than $\pm 2°$ and less than $\pm 0.5°$, respectively, so in most cases it is sufficient to use the θ and ζ values at the scene center.

Before showing examples, here is a short overview of phenomena that influence the surface roughness. The main source of surface roughness is the wind; it generates ripples and waves on the water surface. Apart from spatial variations of the wind field, the following phenomena can modulate the existing roughness:

- Surface films and slicks – they very effectively dampen surface waves and thus reduce the surface roughness (see, e.g., Alpers and Hühnerfuss, 1989). Surface slicks can be caused by oil spills, but they can also be produced by sea organisms such as algae.
- Current gradients – they cause local convergence or divergence of the water surface, thus enhancing or reducing, respectively, the surface roughness. Current gradients can, e.g., be caused by a current flowing over varying depth (see, e.g., Hennings et al., 1988).
- Internal waves – they produce convergence and divergence patterns, such that there are bands of increased and reduced surface roughness (see, e.g., Alpers, 1985).
- Ship wakes – the turbulent wake in the track of the ship usually has a smoother water surface than the surroundings (see, e.g., Melsheimer et al. , 1999).

3. DISCUSSION

We shall now try to apply the theoretical considerations of the previous section to SPOT images. First we plot the relative sun glitter radiance for the two images shown in the introduction (Figures 1 and 2). The first one (Figure 3) indeed shows that the sun glitter radiance has a maximum at very low roughness (small mean square slope) and decreases toward higher roughness (large mean square slope). This explains why oil slicks look bright in that image. The tilt angle for specular reflection of sunlight into the sensor, $\hat{\beta}$, is 3.7°. In contrast, the second one (Figure 4) shows increasing sun glitter radiance with increasing roughness, such that oil slicks look dark; here, $\hat{\beta} = 11.7°$. Note that in these and in all the following plots the range of the mean square slope, i.e., from 0.0 to 0.06, is chosen to cover the range of commonly occurring values. A mean square slope above 0.06 would need, e.g., sustained wind of more than 10 m/s (36 km/h, 20 knots) and is quite unlikely under fair or clear weather conditions (which are necessary to see the sea surface in a SPOT image) in this region.

Figure 5 shows a SPOT image of internal waves in the Andaman Sea, acquired on 30 March, 1998, at 4:20:01 UTC. The roughness bands caused by several groups of internal waves appear dark, which is consistent with the plot of the sun glitter radiance in Figure 6. The tilt angle for specular reflection of sunlight into the sensor, $\hat{\beta}$, is 4.9°.

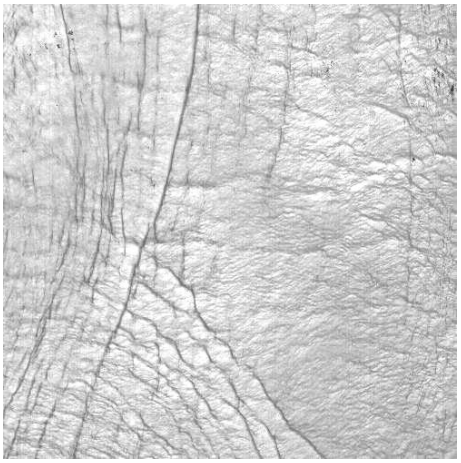

Figure 5: SPOT panchromatic image, 30 Mar 1998, 4:20:01 UTC, Andaman Sea. It shows a superposition of several groups of internal waves that look like dark lines. © CNES 1998

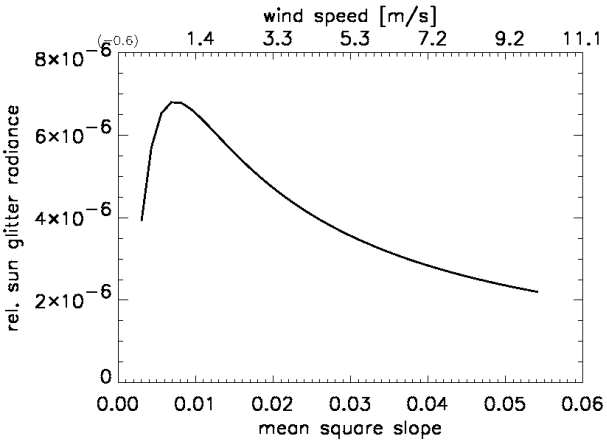

Figure 6: Plot of the relative sun glitter radiance for the SPOT image on the left with dark internal waves (Figure 5); $\hat{\beta} = 4.9°$.

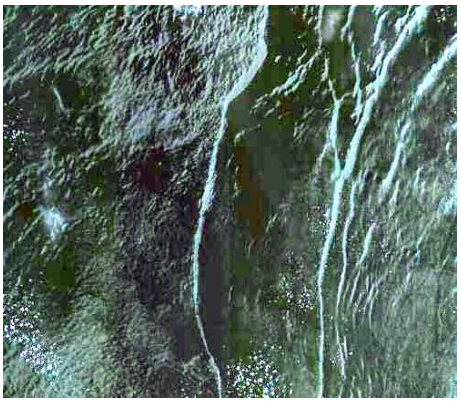

Figure 7: SPOT multispectral image, 31 Aug 1999, 02:57:34 UTC, South China Sea near Pratas/Dongsha Island. It shows a strong internal waves that look like bright. © CNES 1999

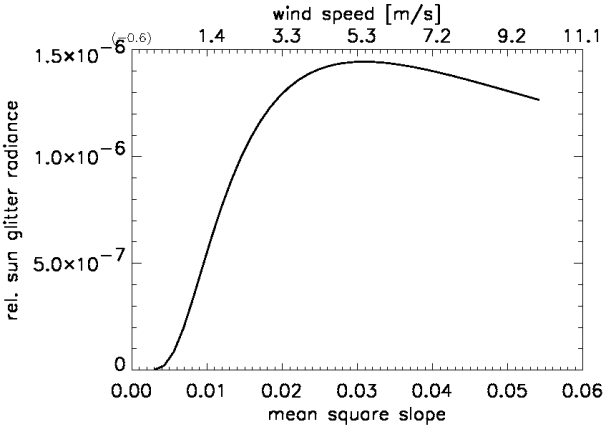

Figure 8: Plot of the relative sun glitter radiance for the SPOT image on the left with bright internal waves (Figure 7); $\hat{\beta} = 9.9°$.

The contrasting case can be seen in Figure 7, a SPOT image acquired on 31 August, 1999, at 02:57:34 UTC, which shows a group of large internal waves in the South China Sea near Pratas (Dongsha) Island. Here the roughness bands appear bright, consistent with the plot in Figure 8. The tilt angle for specular reflection of sunlight into the sensor, $\hat{\beta}$, is 9.9°.

For comparison, the next Figure shows a SPOT image acquired under conditions where the sun glitter radiance can be expected to be very small. Figure 9 was acquired on 22 January, 2000, at 03:32:39 UTC, over the Port Klang area on the West coast of West Malaysia. The tilt angle for specular reflection of sunlight into the sensor, $\hat{\beta}$, is 30.5°; in other words, the maximum of the sun glitter radiance is at very high mean square slope values (beyond the mean square slope range of the plot) as can be seen from the plot (Figure 10). Since the maximum is so far beyond the range of commonly occurring mean square slopes, the values of the sun glitter radiance are very low, about 2 to 3 orders of magnitude smaller than the sun glitter radiance values in all previous examples. The the contribution of the sun glitter radiance to the radiance measured by the sensor is therefore negligible, and the main contributions come from the water column and the sea bottom as well as from the atmosphere (path radiance). The varying brightness and hue of the water in this scene is caused by varying depth and possibly turbidity. In other words, here, unlike in the other scenes shown above, the SPOT sensor can look through the water surface. This is a necessary condition for extracting information on the depth and turbidity of the water from an image.

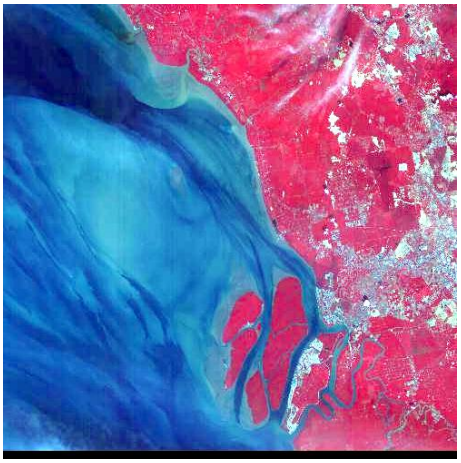

Figure 9: SPOT multispectral image,22 Jan 2000, 03:32:39 UTC, Port Klang, Malaysia. No sun glitter patterns of surface phenomena visible.© CNES 2000

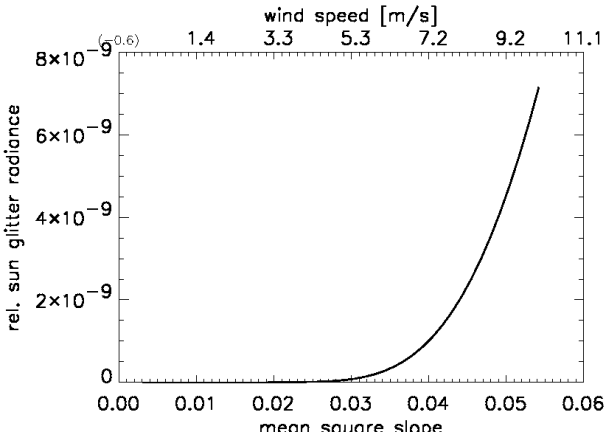

Figure 10: Plot of the relative sun glitter radiance for the SPOT image on the left with no sun glitter patterns (Figure 9); $\hat{\beta} = 30.5°$.

4. SUMMARY AND CONCLUSION

Analyzing the SPOT scenes shown in this paper as well as about 30 other SPOT scenes, we can summarize as follows:

- If the peak of the sun glitter radiance curve is at very low roughness (mean square slope, σ^2 less than about 0.01), or, equivalently, the tilt angle for specular reflection of sunlight into the sensor, $\hat{\beta}$, is below about 6°, smooth areas of the ocean appear bright in SPOT images, and rough areas appear dark. This means, e.g., that surface slicks are bright, and the roughness bands associated with internal waves are dark.
- If the peak of the sun glitter radiance curve is at mean square slopes between about 0.02 and 0.06, or, equivalently, the tilt angle for specular reflection of sunlight into the sensor, $\hat{\beta}$, is between about 8°and 13°, smooth areas of the ocean appear dark in SPOT images, and rough areas appear bright. This means, e.g., that surface slicks are dark, and the roughness bands associated with internal waves are bright.
- If the peak of the sun glitter radiance curve is at mean square slopes between about 0.01 and 0.02, or equivalently, the tilt angle for specular reflection of sunlight into the sensor, $\hat{\beta}$, is between about 6°and 8°, smooth and rough areas of the ocean can appear equally dark, whereas areas with roughness in between are brighter. This means that a qualitative interpretation is difficult without exact knowledge of the in situ roughness parameters.
- Finally, if the peak of the sun glitter radiance curve is at high roughness (mean square slope above 0.1), or, equivalently, the tilt angle for specular reflection of sunlight into the sensor, $\hat{\beta}$, is above about 17°, the sun glitter radiance for commonly occurring ocean surface roughness values is very small, and it can be neglected in SPOT images of tropical oceans. This means that ocean surface phenomena like, e.g. surface slicks and the roughness bands associated with internal waves are invisible, and the SPOT sensor "sees" the water column.

The limiting values given in this summary are only a general guideline, but they should be very useful in interpreting a given SPOT scene or for assessing if a given scene is suitable for extracting information about the water column from it. The findings presented in this paper do in principle also apply to images from other spaceborne optical sensors like Landsat or IKONOS.

ACKNOWLEDGMENTS

We would like to thank W. Alpers for his comments and suggestions.

APPENDIX

A.1 Calculation of tilt and reflection angles for specular reflection

For a given viewing direction of the sensor and a given position of the sun, we want to calculate (1) by which angle $\hat{\beta}$ the water surface has to be tilted in order to cause specular reflection of sunlight into the sensor; and (2) what is the local reflection angle $\hat{\omega}$ for specular reflection of sunlight by a water surface thus tilted. This is a relatively simple

problem of spherical trigonometry, we here give the result for the HRV sensor on the SPOT satellites. The parameters that accompany the data of a SPOT scene are the the scene orientation, τ, which is the azimuth angle of the satellite track; the incidence angle, θ, which is the (off-nadir) viewing angle; the sun azimuth angle, ϕ; and the sun elevation angle which 90°minus the sun zenith angle ζ. We then get:

$$\cos(2\hat{\omega}) = \cos\theta\cos\zeta + \sin\theta\sin\zeta\sin(\tau - \phi) \tag{4}$$

as well as:

$$\cos\hat{\beta} = \frac{\cos\theta + \cos\zeta}{2\cos\hat{\omega}} \tag{5}$$

REFERENCES

Alpers, W., 1985. Theory of radar imaging of internal waves. Nature, 314, pp. 245-247.

Alpers, W., and H. Hühnerfuss, 1989. The damping of ocean waves by surface films: a new look at an old problem. J. Geophys. Res., 94, pp. 6251-6265.

Cox, C., and W. Munk, 1954. Measurement of the roughness of the sea surface from photographs of the sun's glitter. J. Opt. Soc. Am., 44 (11), pp. 838-850.

Hennings, I., R. Doerffer, W. Alpers, 1988. Comparison of submarine relief features on a radar satellite image and on a Skylab satellite photograph. Int. J. Remote Sens., 9 (1), pp. 45-67.

Melsheimer, C., and S.C. Liew, 2001. Extracting bathymetry from multi-temporal SPOT images. This issue (Proceed. 22nd Asian Conference on Remote Sensing, Singapore, Nov. 2001).

Melsheimer, C., H. Lim, C. Shen, 1999. Observation and analysis of ship wakes in ERS SAR and SPOT images. Proceed. 20th Asian Conference on Remote Sensing, Hong Kong, China, pp. 554-559.

Melsheimer, C., H. Lim, L.K. Kwoh, C.M. Shen, M.K.W. Puang, 2000. Signatures of underwater bottom topography in the Straits of Malacca in images from the SPOT satellites. Proceed. IGARSS 2000, Honolulu, Hawai'i, pp. 2684-2686.

Zeisse, C.R., 1995. Radiance of the ocean horizon. J. Opt. Soc. Am. A, 12 (9), pp. 2022-2030.